International Journal of Environmental Science and Technology (2025) 22:6711–6728
https://doi.org/10.1007/s13762-024-06044-2

ORIGINAL PAPER

Utilization and optimization of a sustainable environmental process for simultaneous recovery of H_3BO_3 and NaOH from tincal

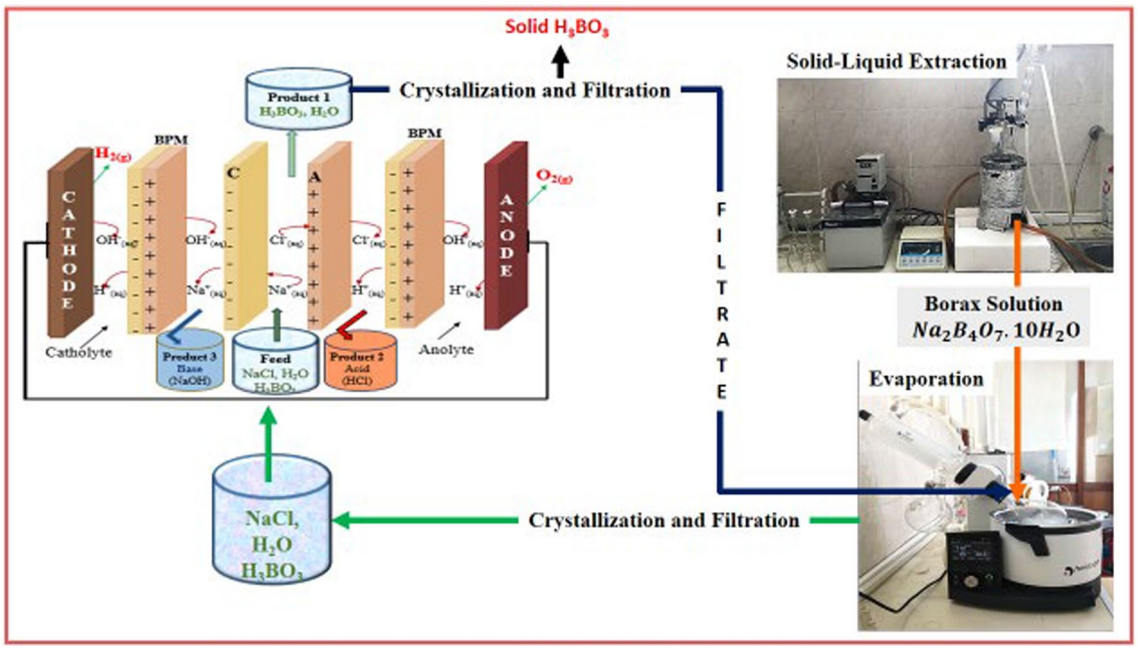
H. Şenol[1] · D. Adıgüzel[1] · A. Kanca[1] · O. N. Ata[1] · S. Yapıcı[2]

Received: 24 May 2024 / Revised: 21 August 2024 / Accepted: 11 September 2024 / Published online: 1 October 2024
© The Author(s) under exclusive licence to Iranian Society of Environmentalists (IRSEN) and Science and Research Branch, Islamic Azad University 2024

Abstract

The present study proposes a bipolar membrane electrodialysis (BMED) integrated sustainable environment-friendly process for producing H_3BO_3 in high purity and NaOH from tincal. Employment of Taguchi experimental design technique supported by TOPSIS optimization method revealed that the optimum process parameters are the initial feed concentration of 160 g NaCl/L and 36 g H_3BO_3/L, the applied current of 4.2 A, the flow rate of 31 L/h, the initial acid and base concentration of 0.15 M, and the electrolyte concentration of 0.2 M. In the experiment performed under optimum operating conditions, 2.15 M acid and 2.20 M base were obtained. The produced acid solution was determined to contain 10.5 g NaCl/L and 2.8 g H_3BO_3/L and the base to contain 13.3 g NaCl/L and 6 g H_3BO_3/L. The boric acid crystals obtained by the crystallization of concentrated feed solution from BMED were determined to have 99.96% purity, which verifies that H_3BO_3 in high purity can be produced by BMED process. Solid waste and concentrated liquid waste formation of the conventional H_3BO_3 production process can also be eliminated, and NaOH can be produced at an industrial scale without chlorine gas emission, by using BMED as an alternative to conventional methods.

Graphical abstract



Editorial responsibility: S. Mirkia.

Extended author information available on the last page of the article

Keywords Bipolar membrane electrodialysis · Boric acid · Desalination · NaOH · Optimization

Introduction

Eti mining enterprises reports that Turkey has the largest boron reserves in the world with a share of 73% (SGD 2018). Boron compounds are mainly used in glass, ceramic and fertilizer industries, and the increasing use of boron-containing products like detergent and fuel, and their use as raw materials for many other industrial areas have continuously expanded the use of boron compounds. Tincal and colemanite are the major boron minerals in Turkey. To obtain boron compounds conventionally, the initial step is the dissolution of the mineral in inorganic and/or organic solvents. After dissolving the mineral, an appropriate separation process is applied to produce boric acid (H_3BO_3). Repeated crystallization followed by washing is the most commonly used separation process. However, the conventional methods result in excessive acid and water utilization, undesired salt formation, and the requirement of additional heating and cooling processes. In 1981, Tolun et al. (1981) reported a work on the production of H_3BO_3 and sodium chloride (NaCl) from tincal ($Na_2B_4O_7{\cdot}10H_2O$) dissolved in hydrochloric acid (HCl) solution. The remarkable part of the study was the application of the electrolysis process for the separation. During the electrolysis, sodium hydroxide (NaOH) in the aqueous phase, and Cl_2 and H_2 in the gaseous stream were generated. Furthermore, HCl generated from Cl_2 and H_2 could be used to solve tincal ore again. However, since tincal ore contains some other minerals like calcium, magnesium, and iron, these minerals also pass into the final H_3BO_3 solution. The results of this study revealed that electrolysis is not an efficient process for the separation of H_3BO_3 in high purity (Tolun 1981). Similar to the electrolysis method, a membrane electrodialysis process was employed for the simultaneous production of NaOH, HCl, NaCl, and H_3BO_3 from tincal. In that case, the low ionization of H_3BO_3 limited its separation by electrodialysis. Nonionization of H_3BO_3 under acidic condition and the relatively lower transportation rate of $B(OH)_4^-$ ions under alkaline conditions were defined as the main challenges to the electrodialysis process. Bipolar membrane electrodialysis (BMED) technology was recently evaluated as a new electrochemistry-based separation process for boron removal. The common findings of the boron removal by BMED process are that the alkaline conditions and low boron concentration in feed solutions were necessary (Nagasawa et al. 2011; Bunani et al. 2017a, b; Noguchi et al. 2018). When the performance of the electrodialysis and BMED processes was compared, the boron removal efficiency was reported to be > 90% for BMED and between 35–45% for electrodialysis. The boron removal takes place in three steps in BMED system. In the first step, the ionization of H_3BO_3 takes place by water dissociated in the bipolar membrane (BPM). The second step is the migration of $B(OH)_4^-$ ions through anion exchange membrane (AEM). In the third step, $B(OH)_4^-$ ions react with proton (H^+) generated in BPM to produce boric acid again (Nagasawa et al. 2011). The alkaline condition can be met by the produced base in the base compartment of BMED system. However, when boron removal from the feed solution with high boron concentration is desired, the BMED is no longer applicable.

The present work aims to overcome the problem of the feed having high boron concentration for the boric acid recovery by BMED technique. In this study, the extraction of tincal ore in water followed by the reaction with HCl was conducted as usual. However, unlike the applications of BMED in the previous work, a modified approach with three steps can be applied by keeping H_3BO_3 in diluate instead of its ionization, transition and reaction. In our previous study, desalination and H_3BO_3 purification, and acid and base recovery under acidic conditions were performed simultaneously. When the applicability of BMED technique was investigated, the performance criteria of BMED, such as desalination ratio, H_3BO_3 purity, acid and base formation, product-based salt conversion, specific energy consumption, and current efficiency were evaluated by taking into account the experimental parameters of the initial amount of H_3BO_3 in the feed and the flow rates of the solutions (Kanca et al. 2022). Under acidic conditions, the dissolution products of tincal are NaCl and H_3BO_3. BMED system was employed for the simultaneous desalination, acid (HCl) and base (NaOH) recovery, resulting in H_3BO_3 purification in diluate. The outputs of this study revealed that BMED process made possible both the enrichment of H_3BO_3 in feed tank at high yields and the recovery of HCl and NaOH (Kanca et al. 2022). The results indicated that desalination was

completed, and H_3BO_3 purity was higher than 95% for all different initial concentrations of H_3BO_3.

The number of performance criteria and experimental parameters have been expanded in this study. H_3BO_3 concentration in feed, molar concentration of acid and base, salt-based acid and base conversion, energy consumption, current efficiency, and processing time are defined as performance indicators of BMED system. The initial concentrations of feed ($NaCl + H_3BO_3$) to BMED, acid, base, and electrolyte, the initial applied current, and the flow rate of solutions were selected as experimental parameters affecting the performance indicators. The results of the preliminary tests and literature mentioned above lead to the determination of 5 experimental parameters and their 4 levels. The performance indicators are defined as the optimization criteria of the process, while the experimental variables are the optimization parameters or control factors. Thus, it was decided to study the optimization of simultaneous desalination, H_3BO_3 recovery in diluate, and NaOH and HCl production by using BMED technique. Before the optimization was carried out, the experiments were first designed by the Taguchi method, which is a widespread method in industrial applications to improve product quality, yield, and the production process. As this method is used to design the experiments for investigating a process, the best level of the experimental parameters is defined by orthogonal arrays (Tong et al. 2003; Gauri et al. 2011; Ata et al. 2017), and the signal-to-noise (SN) ratio is used for the evaluation of the performance criteria. Although Taguchi method is employed for single-response problems, it is not sufficient for both simultaneous solutions of multi-response problems and the derivation of correlations among the responses due to the complicated mathematics (Tong et al. 2004, 2005; Gauri et al. 2011). The overall performance index (OPI) of multiple responses is determined by the **t**echnique for **o**rder **p**reference by **s**imilarity to an **i**deal **s**olution (TOPSIS). The maximum OPI value is identified by using the optimal combination of factors and levels. The calculation details of TOPSIS are explained in part 2.4.

In summary, this study aims to indicate whether BMED can be a promising technology for the simultaneous H_3BO_3 and NaOH recovery from tincal. The work was planned as follows: i. the definition of performance indicators of process, experimental variables, and their levels, ii. the design of the experiments by Taguchi method and performing the experiments, and iii. the evaluation of the findings of the experiments by TOPSIS analysis. Within the framework of this aim and plan, all the performance criteria were discussed by taking into account S/N ratios, and the single optimum condition for all the criteria was determined as the output of the multi-criteria decision-making analysis.

Materials and methods

Reagents and membranes

All the solutions of NaCl and H_3BO_3 for the feed tank, HCl for the acid tank, NaOH for the base and electrolyte tanks were prepared with the chemicals supplied by Merck Company. The PCCell BED 1–4 model BMED system equipped with the online control and data acquisition units was provided by PCCell GmbH, Heusweiler, Germany. The company also supplied anion exchange (PC Acid 60), cation exchange (PC SK) and bipolar membranes, and spacers (ED 640004) for BMED cells. A DC power supply was employed for the appropriate current–voltage application. The main anode and cathode components consisted of the mixed metal oxides coated with titanium. The BMED membrane bundle consisted of cells with 5 repeats. Each cell has three compartments having ion exchange membranes, bipolar membranes and spacers. A total of 17 compartments were formed in the BMED membrane bundle with 5 anion and 5 cation exchange membranes, 6 bipolar membranes and 17 spacers. The characteristics of the ion exchange and bipolar membranes can be found in our previous study (Öner et al. 2023).

Definition of experimental setup and BMED experiments

The whole process proposed for H_3BO_3 and NaOH production from tincal by BMED method can be defined in three steps, as summarized in Fig. 1. The first step is the extraction of tincal with water. During this step, tincal is dissolved into water as borax ($Na_2B_4O_7{\cdot}7H_2O$), while most of the impurities in the ore are precipitated. In the second step, the chemical reaction between borax and HCl produces H_3BO_3 and NaCl. Then, evaporation and crystallization followed by filtration are applied to obtain crystalized H_3BO_3 in the third step of the process. After the separation of the solid filtrate of H_3BO_3, the solution including H_3BO_3, NaCl and H_2O is fed to BMED system. The in-situ HCl production in BMED process eliminates the acid cost that is needed for the reaction with tincal. In addition to acid recovery, liquid waste-free desalination and base recovery can also be considered as

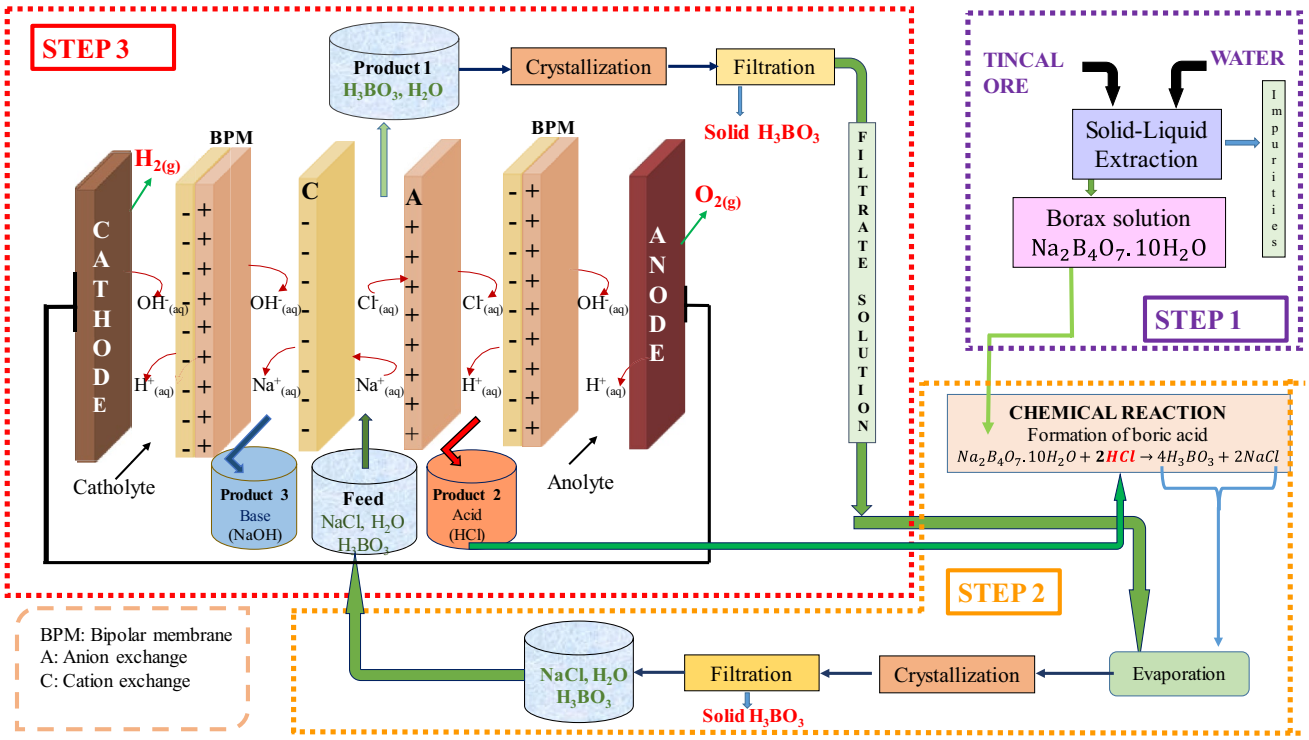


Fig. 1 Experimental setup and flow chart of whole process

the environmental and economic advantages of the BMED technology. This work is related to the determination of the optimum working conditions for the third step.

Table 1 Parameters and their levels

Parameter		Parameter levels			
		1	2	3	4
A	Initial NaCl + H_3BO_3 (g/L)	120 + 36	140 + 36	160 + 36	180 + 36
B	Current (A) at 20 V	3.2	4.2	5.2	6.2
C	Flow rate (L/h)	10	17	24	31
D	Initial acid & base (M)	0.05	0.1	0.15	0.2
E	Initial electrolyte (M)	0.05	0.1	0.15	0.2

The feed, acid, base, and electrolyte tanks were initially filled with 1 L of simulated solutions. The temperature of the solutions was kept constant at 25 °C ± 1 by using jacketed tanks with thermostat. The experiments were terminated when the conductivity of the solution in the feed tank was reduced below 2 mS/cm. The performance indicators of BMED systems were chosen as H_3BO_3 concentration in the feed, the concentration of acid and base, salt-based acid and base conversion, current efficiency, impurities in acid and base, running period, and energy consumption. Since the initial concentrations of feed, acid and base, and electrolyte, the initially applied current, and the flow rate of solutions affect the performance indicators, these variables were selected as the experimental parameters. An experimental design with 4 levels and 5 parameters was employed for the optimization of the process. The parameters and their levels are presented in Table 1.

Data analysis

During the BMED process, the concentrations of acid, base and H_3BO_3 in the related tanks were determined by wet chemical analysis. All details of the wet analysis methods were explained in our previous study (Kanca et al. 2022). The change in the conductivity of the feed tank was recorded automatically by the system hardware and software. The desalination, boric acid concentration, acid and base concentration, conversion to acid/base, energy consumption, current efficiency, and product purity were selected as the process performance criteria for the BMED process.

The desalination was determined by using the following equation:

$$\%\ \text{Desalination (De)} = \frac{\sum C_{ion,t}}{C_{salt,o}} \times 100 \quad (1)$$

where $\sum C_{ion,t}$ is the total ion concentration at the end of the experiment (g/L), and $C_{salt,o}$ the initial salt concentration (g/L).

The final boric acid concentration (g/L) was calculated by equation of;

$$\text{Final Boric Acid (H3BO3) concentration} = \frac{C_{i,t}}{V_{i,t}} \quad (2)$$

where $C_{i,t}$ is the final boric acid concentration amount (g), and $V_{i,t}$ final diluate volume (L).

The acid/base concentration (mole/L) was calculated by;

$$\text{Final acid and base concentration} = \frac{n_{i,t}}{V_{i,t}} \quad (3)$$

where $n_{i,t}$ is the final acid or base amount (mole), and $V_{i,t}$ final acid or base volume (L).

The conversion to acid or base was found by using following expression:

$$\%\,\text{Conversion} = \frac{C_{i,t} - C_{i,o}}{C_{total}} \times 100 \quad (4)$$

where $C_{i,t}$ is the final acid or base concentration (mole/L) $C_{i,o}$ the initial acid or base concentration (mole/L), and C_{total} the total acid or base concentration for the total salt conversion (mole/L).

The specific energy consumption (kW.h/kg) was calculated based on applied current/voltage and feed weight.

$$\text{Energy consumption (E)} = \frac{1}{m} \times \int_0^t V \times I \times dt \quad (5)$$

where m is the initial feed amount (kg), V the applied potential (V), and I the applied current (A).

The BMED system's current efficiency was determined by considering the proton and hydroxyl ions produced by the dissociation of water on BPM.

$$\%\,\text{Current efficiency } (\eta) = \frac{z \times F}{60 \times N \int_0^t I \times dt} \times \left[(C \times V)_{i,t} - (C \times V)_{i,o}\right] \quad (6)$$

where z is the ion charge of proton or hydroxyl, F is the Faraday constant 96,485 (coulomb/mole), N is the cell number in BMED, I is the applied current (A), $(C \times V)_{i,t}$ is the final molar amount acid or base (mole/L), $(C \times V)_{i,o}$ is the initial molar amount acid or base (mole/L).

The impurity acid or base ($g/L_{solution}$) was calculated by using following equation:

$$\text{Impurity acid or base } (\sum) = C_{\text{boric acid},t} + C_{\text{salt},t} \quad (7)$$

where $C_{\text{boric acid},t}$ is the final boric acid concentration in acid or base tank (g/L), $C_{\text{salt},t}$ is the final salt concentration in acid or base tank (g/L).

After the calculation of the performance values, they were converted to signal-to-noise ratio, and the effects of the performance parameters on the performance criteria were discussed by taking into account S/N ratio. Contrary to computable indicators, processing time and impurities in acid and base tanks are defined as the measurable performance criteria. The processing time is the duration from the beginning of the experiment until the conductivity of the feed salt solution reduces to 2 mS/cm. Since the experiments were performed with simulated solutions, the impurities in the products were just defined as Na^+ in the acidic solution, Cl^- in the basic solution.

The analyses of Na^+ and Cl^- were performed with Thermo Dionex ICS 1100 and Thermo Dionex ICS 3000 ion chromatographies, respectively. To determine the purity of boric acid crystals, 1 g of dried crystal was taken and dissolved in pure water, and the content of the solution was then determined by wet methods (Kanca et al. 2022). Boric acid crystals were also analyzed by an XRD (Empyrean, Panalytical, Almelo, The Netherlands) equipped with monochromatic Cu radiation operated at 40 mA and 45 kV from 5° to 90°.

Statistical analysis

Experimental parameters affecting the performance of the process were defined by Taguchi method. In this method, the signal-to-noise ratio (S/N) can be used to evaluate the quality characteristic of the desired value. The main property of this method is to provide the facility of investigating the parameters affecting the experiments in controllable and/or uncontrollable groups and studying each parameter at more than two levels. The optimum condition is determined by studying the main effects of each factor, indicating the general tendency of the effect of each factor. Since the quality of any obtained products is measured with one criterion or with a combination of more than one criterion, it belongs to one of three situations, independent of the feature of the measurement: larger is better, smaller is better and nominal is better (Kackar 1985; Pignatiello Jr 1988; Ata et al. 2017). When the optimum level of the parameters was determined, if the larger level is better, then, SN ratio is defined as:

$$SN_L = -10\text{Log}\left[\frac{1}{n}\sum_{n=1}^{n}\frac{1}{y^2}\right] \quad (8)$$

where n is the number of repeated experiments and y is the performance criteria value. In this case, the target value of y is infinitive, and the optimum value of the parameter is the one making SN_L maximum. When the smaller level of the parameter can be better for the optimum, SN ratio is defined as:

$$SN_L = -10\text{Log}\left[\frac{1}{n}\sum_{n=1}^{n}y^2\right] \quad (9)$$

In this case, the target value of the quality variable "y" is zero, and the optimum value of the parameter makes SN_S minimum. When the optimum conditions are analyzed, it is found that the parameter levels giving maximum SN_L are the optimum values for H_3BO_3 enhancement, the acid and base concentration, the conversion based on products, and the current efficiency. The parameter levels giving maximum SN_S are the optimum values for the impurities in the products, the energy consumption, and the processing time. When an optimal single response is sufficient for the solution of multi-criteria problems, Taguchi is the favorable optimization method. However, to optimize the multi-response problem, the Taguchi method should be supported by the multi criteria decision making (MCDM) method. The presence of multiple criteria makes a choice-based problem quite complex during the determination of alternatives. At that point, the technique for order preference by similarity to ideal solutions (TOPSIS) can be used to determine both favorable and unfavorable ideal alternatives from the decision matrix. Thus, TOPSIS provides to reach one single optimum response for all criteria. The main steps of TOPSIS are explained below in detail (Tong et al. 2005; Behzadian et al. 2012; Özdagoglu 2013a, b; Panda and Jagadev 2018; Öner et al. 2023).

1. Decision matrix formation: SN values determined by the Taguchi method were used to form a decision matrix.

$$\text{Decision matrix } \left(D_{ij}\right) = \begin{bmatrix} d_{11} & \cdots & d_{1n} \\ \vdots & \ddots & \vdots \\ d_{m1} & \cdots & d_{mn} \end{bmatrix} \quad i = 1, 2, \ldots, m \text{ and } j = 1, 2, \ldots, n$$

2. Normalization of decision matrix: Vector normalization is generally preferred in TOPSIS (Özdagoglu 2013a, b). Equation (10) is employed for the formation of a normalized decision matrix.

$$\text{Normalized decision matrix } \left(\mathcal{N}_{ij}\right) = \begin{bmatrix} \backslash_{11} & \cdots & \backslash_{1n} \\ \vdots & \ddots & \vdots \\ \backslash_{m1} & \cdots & \backslash_{mn} \end{bmatrix}$$

$$\backslash_{ij} = \frac{d_{ij}}{\sqrt{\sum_{i=1}^{m} (d_{ij})^2}} \quad i = 1, 2, \ldots, m \text{ and } j = 1, 2, \ldots, n \tag{10}$$

3. Determination of weight factor of each parameter: Equal weight factors were accepted for each performance criterion. Since the total number of performance criteria is 10, the weight factor (w_i) is 0.1.

w_i is the weight factor of each criterion and $\sum_j = 1^n w_j = 1$

4. Formation of weighted normalized decision matrix: The normalized decision matrix was multiplied by the weight fraction to form the weighted normalized decision matrix.

$$\text{Weighted normalized decision matrix } \left(\mathcal{V}_{ij}\right) = \begin{bmatrix} w_{1\cdot 11} & \cdots & w_{n\cdot n1} \\ \vdots & \ddots & \vdots \\ w_{1\cdot m1} & \cdots & w_{n\cdot mn} \end{bmatrix} \text{or,}$$

$$\left(\mathcal{V}_{ij}\right) = \begin{bmatrix} \sqsubseteq_1 & \cdots & \sqsubseteq_{n1} \\ \vdots & \ddots & \vdots \\ \sqsubseteq_{m1} & \cdots & \sqsubseteq_{mn} \end{bmatrix}$$

5. Formation of positive ideal and negative ideal solutions: To create the ideal solutions, the biggest (for positive ideal) and/or the smallest (for negative ideal) values of the weighted criteria in the weighted normalized decision matrix are put into Eq. 11 and 12, respectively. "n" number of criteria is present in both positive and negative solution sets.

$$\text{Positive ideal solution } \left(\mathcal{S}^+\right) = \left\{\left(\max_i \times_{ij} | j \in J\right), \left(\min_i \times_{ij} | j \in \mathbb{J}\right)\right\} \tag{11}$$

$$\mathcal{S}^+ = \left\{\mathcal{S}_1^+, \mathcal{S}_2^+, \ldots, \mathcal{S}_n^+\right\}$$

$$\text{Negative ideal solution } \left(\mathcal{S}^-\right) = \left\{\left(\min_i \times_{ij} | j \in J\right), \left(\max_i \times_{ij} | j \in \mathbb{J}\right)\right\} \tag{12}$$

$$\mathcal{S}^- = \left\{\mathcal{S}_1^-, \mathcal{S}_2^-, \ldots, \mathcal{S}_n^-\right\}$$

6. Calculation of distance from ideal positive and ideal negative solutions of alternatives: When the distance from the ideal solution is calculated, The Euclidian Distance Approach is applied. Distance from positive ideal solution is determined by Eq. (13), while Eq. (14) is used to determine the distance from negative ideal solution. The number of calculated positive and negative D_i is equal to the number of compared criteria.

$$\text{Distance from positive ideal solution } \left(\mathcal{D}_i^+\right) = \sqrt{\sum_{j=1}^{n} \left(\sqsubseteq_{ij} - \mathcal{S}_j^+\right)^2} \quad (13)$$

$$\text{Distance from negative ideal solution } \left(\mathcal{D}_i^-\right) = \sqrt{\sum_{j=1}^{n} \left(\sqsubseteq_{ij} - \mathcal{S}_j^-\right)^2} \quad (14)$$

7. Calculation of relative distance from ideal negative solution to ideal positive solution: The relative closeness of each alternative to the ideal solution is calculated by using the distance measures from the positive ideal and negative ideal solutions (Eq. 15). When $\mathcal{T}_i = 1$, the related criteria are at the point of positive ideal solution. In the case of $\mathcal{T}_i = 0$, the related criteria are at the point of negative ideal solution.

$$\text{Relative proximity } \left(\mathcal{T}_i\right) = \frac{\mathcal{D}_i^-}{\left(\mathcal{D}_i^- + \mathcal{D}_i^+\right)} 0 \le \mathcal{T}_i \le 1 \quad (15)$$

Results and discussion

Results of experiments

The results of 16 experiments designed according to Taguchi method are presented in Table 2. Each experiment was repeated twice at different times and order. As seen in the table, since experimental parameters have no remarkable effect on desalination, it was not considered as the performance criterion. Instead of desalination, running time was added as an experimental criterion due to its strong dependency on process efficiency. Since the performance criteria are associated with the signal-to-noise ratio (S/N), the effects of the experimental parameters on performance criteria were discussed by taking into consideration S/N values. As a result, S/N values make possible the simultaneous discussion by considering the five experimental parameters with four levels in one graph. Variance analysis was also performed for the amounts of product formed, salt conversions, current efficiency, energy consumption, impurities in the product and test duration. Variance analyzes are given in Tables 8–17 in supplementary file. In these tables, the effectiveness of the parameters for each performance criterion can also be determined. The larger the F value calculated for the relevant parameters, the greater the effectiveness of the parameter. According to variance analysis, the most effective parameters on the performance criteria were the initial salt—H_3BO_3 concentration and current, while the least effective parameter was found to be the effect of the initial electrolyte concentration. Before the decision matrix was formed, ten performance criteria were classified in Table 3 by taking into consideration the maximum and minimum performance criteria (SN_L and SN_S). Equal weight factors were accepted for each performance criterion. Since the total number of performance criteria is 10, the weight factor (w_i) is 0.1. When the decision matrix was formed, Taguchi predictions of SN_S and/or SN_L values for 16 experiments were employed and they are presented in Table 4. After the effects of parameters on performance responses were discussed by taking into consideration S/N values, the remaining steps of TOPSIS were completed to combine the optimum experimental parameters.

Effects of experimental parameters on performance criteria with respect to S/N values

The parameter levels maximizing the S/N_L values are optimum for the final H_3BO_3 concentration in feed, acid and base production, salt-based acid and base conversion, and current efficiency. On the other hand, the parameter levels maximizing the S/N_S values are optimum for the performance indicator of energy consumption, running time, and the amount of impurities.

Boric acid concentration

The final H_3BO_3 concentration in the feed is affected by initial H_3BO_3 and/or salt concentration (A), current (B), flow rate (C), initial acid and base concentration (D), and electrolyte concentration (E). As seen in Fig. 2, among five parameters, the initial H_3BO_3 concentration and current appear to be the most effective parameters on the final H_3BO_3 concentration. S/N values increase with increasing initial (H_3BO_3 + NaCl) concentration and current from level 1 to 4. Since higher NaCl concentrations lead to longer processing time, the amount of water transferred by electro-osmosis from the feed compartment to the acid and base compartments also increases (Tanaka 2004; Ghyselbrecht et al. 2014; Li et al. 2016). Contrary to the effect of the initial NaCl concentration on processing time, increasing current speeds up the process by shortening the processing time. Therefore, faster ion transfer results in a higher concentration gradient between the compartments, and lower electro-osmosis due to short processing period. The increase or decrease of water transport associated with ions transfer from the feed phase to neighboring compartments directly affects the concentration of boric acid in the feed (Jiang et al. 2015; Sun et al. 2017).

As seen in Fig. 2, flow rate, initial acid and base concentration, and electrolyte concentration do not exhibit a regular behavior with the change in parameter level; however, it can be said that the flow rate and electrolyte concentration are not as effective as A and B on the H_3BO_3 concentration in

Table 2 Results of experiments

Exp. No	Level of parameter					H_3BO_3 (g/L)	HCl (M)	NaOH (M)	Desalination (%)	Conversion to acid (%)	Conversion to base (%)	$$\Sigma$$ Impurity in acid (g/L)	$$\Sigma$$ Impurity in base (g/L)	Current efficiency (%)	Energy consumption (kW h/kg)	Running time (min)
	A	B	C	D	E											
1	1	1	1	1	1	51.50	1.58	1.58	98.60	87.10	86.90	6.90	13.10	0.73	2.31	243.00
2	1	2	2	2	2	48.00	1.76	1.73	97.71	92.90	91.40	5.30	9.10	0.82	1.72	180.00
3	1	3	3	3	3	55.40	1.83	1.82	99.04	90.80	90.20	4.70	6.40	0.82	1.82	156.00
4	1	4	4	4	4	56.70	1.87	1.86	99.45	94.10	93.60	4.50	5.10	0.84	1.96	127.00
5	2	1	2	3	4	48.90	1.82	1.83	99.09	82.00	82.70	12.50	20.90	0.75	1.80	278.00
6	2	2	1	4	3	52.80	2.00	2.05	98.63	89.40	91.80	8.80	12.40	0.79	1.75	215.00
7	2	3	4	1	2	61.00	1.78	1.80	99.14	84.20	85.10	9.80	14.10	0.82	2.15	167.00
8	2	4	3	2	1	58.90	1.95	1.92	98.95	86.90	85.60	9.80	10.80	0.76	2.53	157.00
9	3	1	3	4	2	54.90	2.04	2.05	99.32	81.90	82.50	13.90	23.90	0.73	1.89	319.00
10	3	2	4	3	1	62.10	2.15	2.20	99.22	84.10	86.20	13.30	19.30	0.98	1.88	198.00
11	3	3	1	2	4	61.10	2.15	2.16	99.62	87.50	87.90	9.60	13.90	0.78	1.95	210.00
12	3	4	2	1	3	75.50	2.05	2.10	99.60	88.10	90.30	9.10	12.60	0.78	2.25	180.00
13	4	1	4	2	3	54.60	2.09	2.12	99.38	80.90	82.10	20.10	25.40	0.71	1.79	362.00
14	4	2	3	1	4	79.10	2.26	2.20	99.77	86.30	84.10	11.80	17.40	0.74	1.81	300.00
15	4	3	2	4	1	81.10	2.42	2.45	99.75	87.80	89.00	10.50	14.90	0.68	2.72	280.00
16	4	4	1	3	2	74.20	2.55	2.61	99.76	92.90	95.10	5.90	9.30	0.81	2.44	215.00

Table 3 Performance criteria classification with respect to S/N

Performance Criteria	$SN_{(L/S)}$	Weight factor (w)
H_3BO_3 concentration (g/L)	Maximum (SN_L)	0.1
Acid concentration (M)	Maximum (SN_L)	0.1
Base concentration (M)	Maximum (SN_L)	0.1
Conversion to acid (%)	Maximum (SN_L)	0.1
Conversion to base (%)	Maximum (SN_L)	0.1
Current efficiency (%)	Maximum (SN_L)	0.1
Running time (min)	Minimum (SN_S)	0.1
Total impurity in acid (g)	Minimum (SN_S)	0.1
Total impurity in base (g)	Minimum (SN_S)	0.1
Energy consumption (kWh/kg)	Minimum (SN_S)	0.1

diluate. The most important factors which affect the concentration of H_3BO_3 in the final diluate are the transportation of water by electro-osmosis and diffusion of H_3BO_3 into the acid and base compartments. Higher water transportation and lower H_3BO_3 diffusion during the process result in higher boric acid concentration in the final diluate. Increasing salt concentration means the transportation of related species in larger amounts, and naturally, more water with electro-osmosis together with them, concentrating the boric acid in the final solution.

Acid and base production

The effects of five parameters on acid and base production are summarized in Fig. 3a for acid and 3b for base. It was found that initial feed concentration has the strongest effect, while electrolyte concentration and flow rate have little effect on acid and base production. The most important factors affecting the acid and base concentration are common ion transport, back diffusion of products, and water transport from the feed compartment to the acid and base compartment by electro-osmosis (Rottiers et al. 2014; Dursun et al. 2021; Öner et al. 2023). It was determined that the concentration of acid and base produced in the process increased with increasing initial salt concentration. During the process, water molecules in hydrate form are transported from salt compartments to neighboring acid and base compartments together with ions by electro-osmosis under the effect of the electric field. Increasing initial salt concentration leads to increased processing time, and it results in an increase in the transfer of water from the salt compartment to neighboring compartments by electro-osmosis. Therefore, this phenomenon leads to an increase in the volume of acid and base solutions, while a decrease in the volume of salt solution (Tanaka 2004; Ghyselbrecht et al. 2014; Li et al. 2016). Water transport by electro-osmosis is the major factor limiting the concentration of acid and base produced. Applied current and initial acid and base concentration have similar effects on acid and base production during the process. Increasing salt concentration causes higher ion transfer through acid and base compartments, resulting in higher acid and base production. Increasing the flow rate also appears to have a small effect on acid and base production.

Acid and base conversion

Acid and base conversion is another performance criterion of the process, and Fig. 4 indicates that almost all the parameters except electrolyte concentration affect the acid and base conversion. S/N values of acid and base conversion vary between 39.2 and 38.3. Since the larger S/N values are better for acid and base conversion, the highest S/N is favorable for both. Therefore, except for initial H_3BO_3 and flow rate, the highest current (B), and concentration of acid and base (D) can be preferred for the highest S/N. The effect of electrolyte concentration does not seem to be very distinctive on acid and base conversion. Increasing initial salt concentration increases the processing time, the amount of product formed, water transport by electro-osmosis from the salt compartment to the product compartments, and the reverse flux of ions from the product compartments to the salt compartment towards the end of the experiment. As shown in the figure, these situations result in a decrease in product-based salt conversion with increasing initial salt concentration. Increasing current density accelerates ion transport by migration, reduces the reverse ion diffusion from the acid and base compartments into the salt compartment towards the end of the experiment, and shortens the time of processing leading to increased salt conversion (Fu et al. 2014; Ghyselbrecht et al. 2014; Rottiers et al. 2014; Li et al. 2016). The migration of ions under an electrical field is the most important transfer mechanism of the electro-membrane process. Diffusion, advection, and electro-osmosis are the other ionic and molecular transfer mechanisms taking place during the process. The increase in bulk flow rate contributes to the transfer of ions from bulk to the surface of membranes. A spacer is used both to create a compartment between charged membranes and to direct the solutions through the related compartments. The spacers between the membranes allow ions to reach the relevant place by preventing the contact of membranes with each other. The presence of spacers, on the other hand, causes both turbulence and increased flow resistance. However, the flow of ions through the membrane is not affected by increasing bulk flow rate since the membrane is closed to hydrodynamic effects.

Although increasing bulk flow can affect the advection (drag of ions) positively, the effect of advection is negligible compared to migration (Kanca et al. 2022). However, as can be seen in Fig. 4a and b, when the flow rate increases, the

Table 4 Decision matrix formed by Taguchi's predictions of SN values

Exp. no	H_3BO_3 (g/L)	Conc. Acid (M)	Conc. Base (M)	Conversion to acid (%)	Conversion to base (%)	Current efficiency (%)	∑ Impurity in acid (g)	∑ Impurity in base (g)	Energy consumption (kW h/kg)	Running time (min)
S/N	Max	Max	Max	Max	Max	Max	Min	Min	Min	Min
1	34.24	3.91	3.86	38.80	38.78	− 2.73	− 16.78	− 22.35	− 7.27	− 47.71
2	33.62	4.72	4.71	39.36	39.22	− 1.72	− 14.49	− 19.18	− 4.71	− 45.11
3	34.87	5.16	5.01	39.16	39.10	− 1.72	− 13.44	− 16.12	− 5.20	− 43.86
4	35.07	5.29	5.22	39.47	39.43	− 1.51	− 13.06	− 14.15	− 5.85	− 42.08
5	33.79	5.18	5.09	38.28	38.35	− 2.50	− 21.94	− 26.40	− 5.11	− 48.88
6	34.45	5.99	6.18	39.03	39.26	− 2.05	− 18.89	− 21.87	− 4.86	− 46.65
7	35.71	4.58	5.06	38.51	38.60	− 1.72	− 19.82	− 22.98	− 6.65	− 44.45
8	35.40	5.63	5.49	38.78	38.65	− 2.38	− 19.82	− 20.67	− 8.06	− 43.92
9	34.79	6.13	6.11	38.27	38.33	− 2.73	− 22.86	− 27.57	− 5.53	− 50.08
10	35.86	6.47	6.85	38.50	38.71	− 0.18	− 22.48	− 25.71	− 5.48	− 45.93
11	35.72	6.52	6.69	38.84	38.88	− 2.16	− 19.65	− 22.86	− 5.80	− 46.44
12	37.56	6.22	6.41	38.90	39.11	− 2.16	− 19.18	− 22.01	− 7.04	− 45.11
13	34.74	6.39	6.43	38.16	38.29	− 2.97	− 26.06	− 28.10	− 5.06	− 51.17
14	37.96	7.02	6.72	38.72	38.50	− 2.62	− 21.44	− 24.81	− 5.15	− 49.54
15	38.18	7.39	7.75	38.87	38.99	− 3.35	− 20.42	− 23.46	− 8.69	− 48.94
16	37.41	7.91	8.23	39.36	39.56	− 1.83	− 15.42	− 19.37	− 7.75	− 46.65

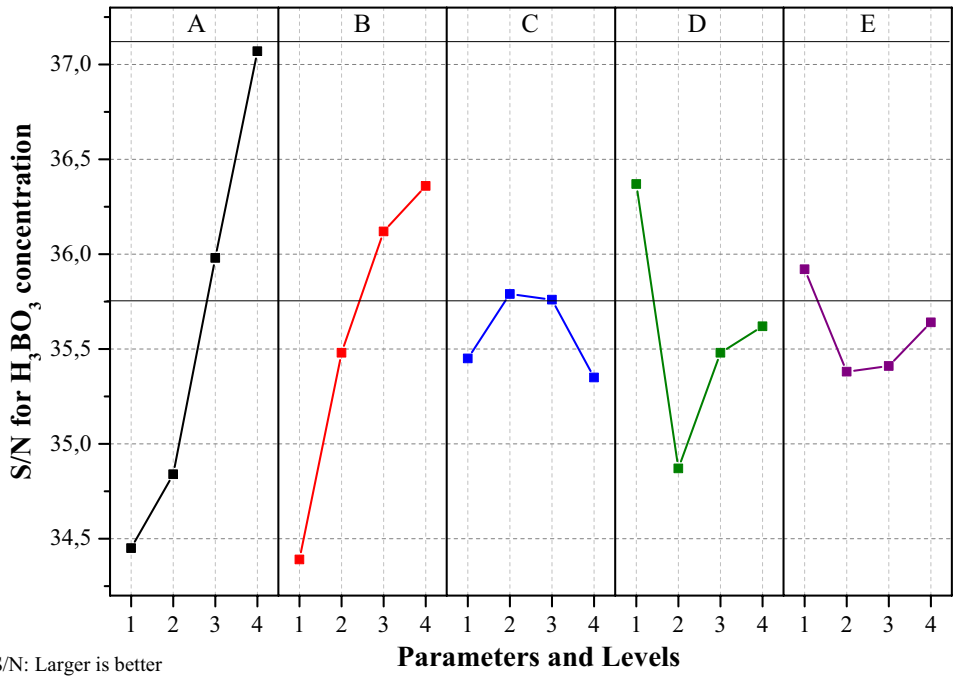


Fig. 2 Effects of parameters on H_3BO_3 concentration

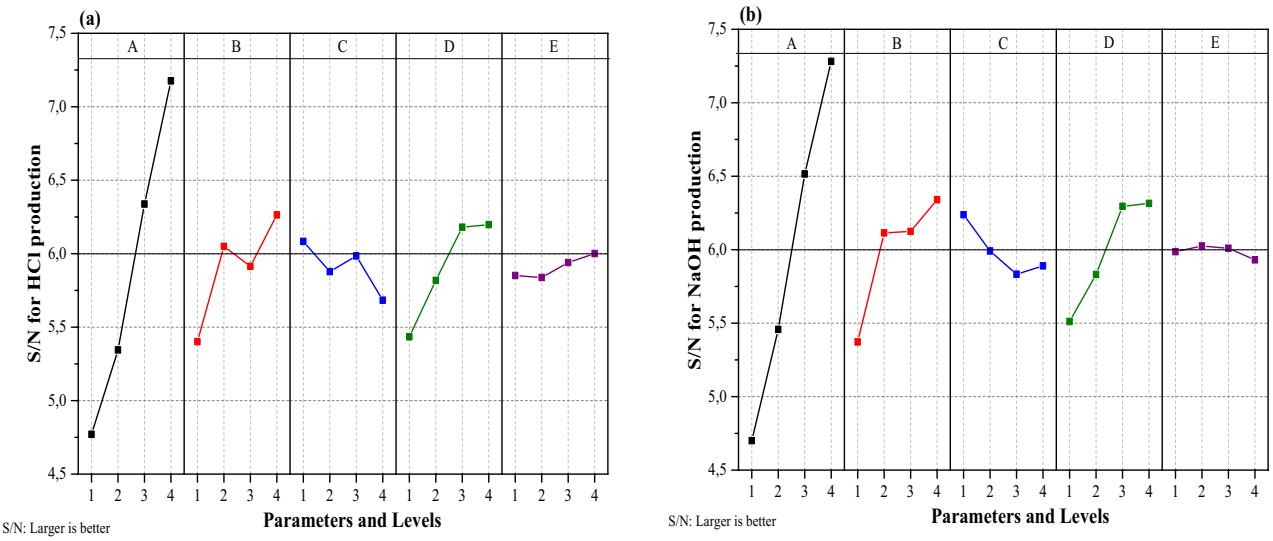


Fig. 3 Signal-to-noise ratio for acid (**a**) and base (**b**) production

common ion transport increases, and the conversion of salt to acid and base decreases.

Impurity in acid and base

Since the smaller S/N values are favorable for impurity, the levels of parameters making S/N lowest should be chosen. Figure 5 indicates that the most effective parameters on impurity are initial feed concentration, current, and flow rate. The co-ion transfer is one of the most important reasons for impurity (Ghyselbrecht et al. 2014). The undesired ion transfer increases when the processing time increases. Since the decrease in initial NaCl concentration and flow rate results in a decrease in processing time, impurity in acid

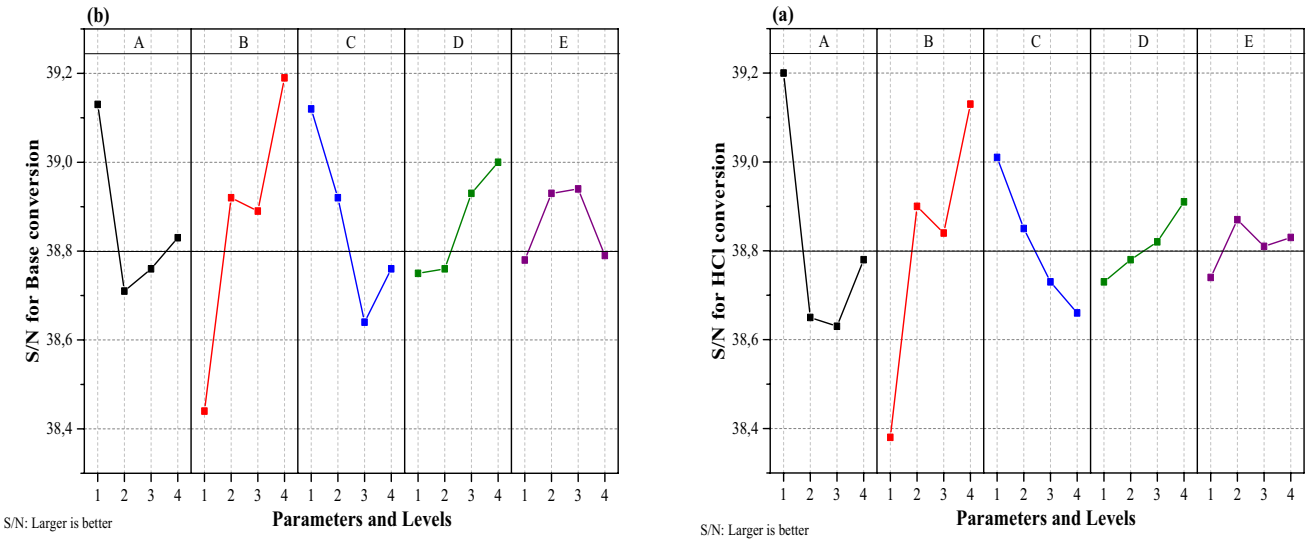


Fig. 4 Signal-to-noise ratio for acid (**a**) and base (**b**) conversion

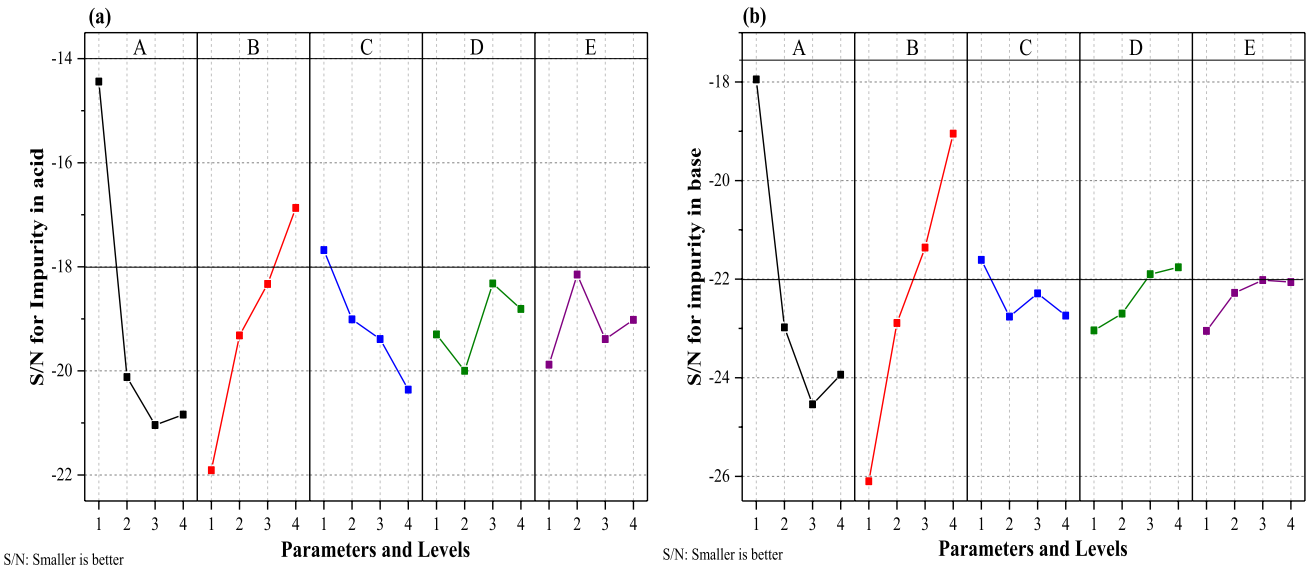


Fig. 5 Signal-to-noise ratio for impurity in acid (**a**) and in base (**b**)

and base tanks decreases. The diffusion of H_3BO_3 is another reason for impurity in acid and base tanks. Long processing time enhances the H_3BO_3-based impurity (Kanca et al. 2022). Contrary to the effect of initial salt concentration and flow rate, increasing current decreases the impurity.

Level 4 of parameters A and C and level 1 of parameter B look like as good preferences for the lowest impurity. D and E appear less effective than A, B, and C. As shown in Fig. 5a and b, boric acid transport from the feed compartment to neighboring compartments increases with increasing flow rate, enhancing the concentration of impurities in the product (Kanca et al. 2022).

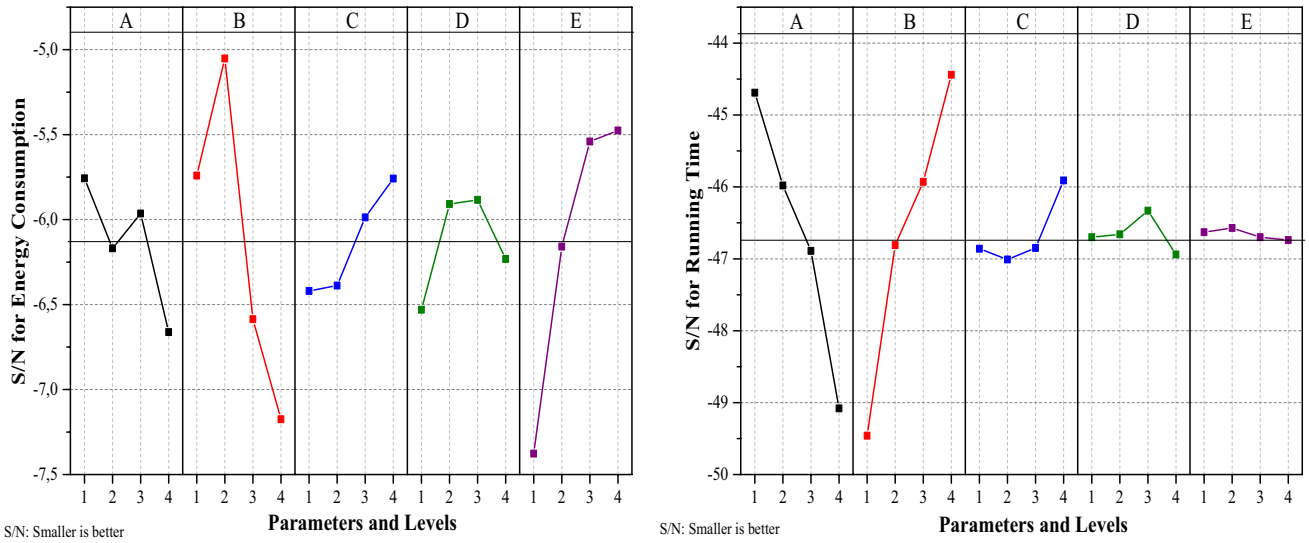


Fig. 6 Signal-to-noise ratio for energy consumption (**a**) and running time (**b**)

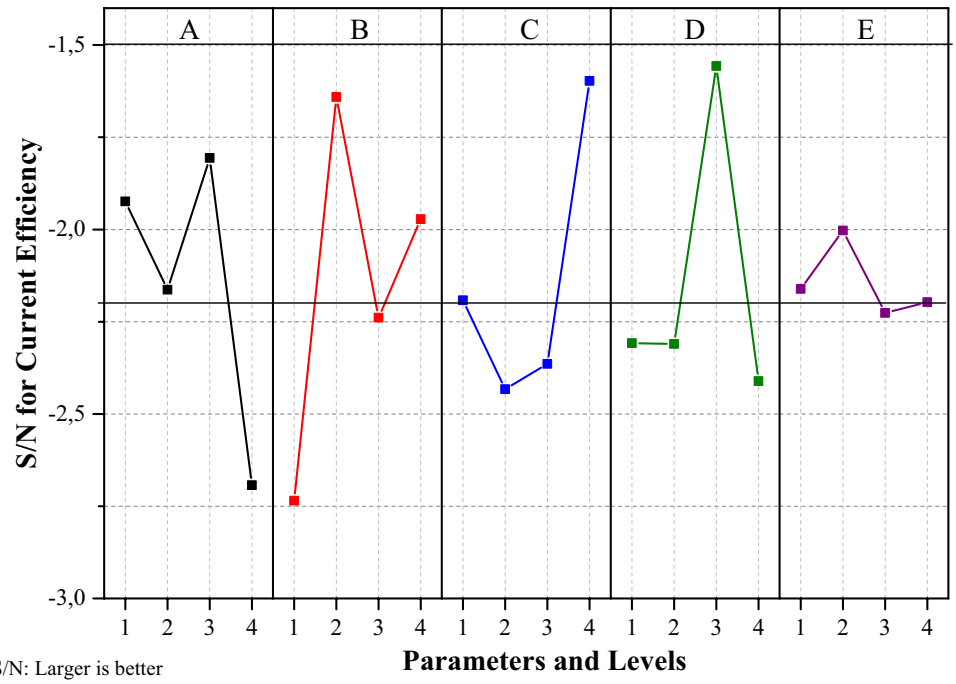


Fig. 7 Signal-to-noise ratio for current efficiency

Energy consumption and running time

Energy consumption and running time are the most important parameters indicating the process feasibility. Figure 6a shows that the current and electrolyte concentration affect energy consumption more than the other parameters. When the running time was examined, Fig. 6b reveals that A and B are very effective on running time. However, the flow rate, the initial acid and base concentration, and electrolyte concentration on S/N for running time are not as effective as the initial feed concentration and current. As seen in Fig. 6a, the electrolyte concentration affects the

Table 5 Weighted and normalized decision matrix

	H_3BO_3	HCl	NaOH	Conversion to acid	Conversion to base	∑ Impurity in acid	∑ Impurity in base	Current efficiency	Energy consumption	Running Time
Weight fraction	0.1	0.1	0.1	0.1	0.1	0.1	0.1	0.1	0.1	0,1
Experiment										
	Max	Max	Max	Max	Max	Min	Min	Max	Min	Min
1	0.0240	0.0163	0.0158	0.0250	0.0249	−0.0216	−0.0247	−0.0302	−0.0290	−0.0255
2	0.0236	0.0197	0.0193	0.0254	0.0252	−0.0186	−0.0212	−0.0190	−0.0188	−0.0241
3	0.0245	0.0215	0.0206	0.0252	0.0252	−0.0173	−0.0178	−0.0190	−0.0208	−0.0235
4	0.0246	0.0220	0.0214	0.0254	0.0254	−0.0168	−0.0156	−0.0167	−0.0233	−0.0225
5	0.0237	0.0216	0.0209	0.0247	0.0247	−0.0282	−0.0291	−0.0276	−0.0204	−0.0262
6	0.0242	0.0250	0.0254	0.0251	0.0253	−0.0243	−0.0241	−0.0226	−0.0194	−0.0250
7	0.0251	0.0191	0.0208	0.0248	0.0248	−0.0255	−0.0254	−0.0190	−0.0266	−0.0238
8	0.0249	0.0235	0.0226	0.0250	0.0249	−0.0255	−0.0228	−0.0263	−0.0322	−0.0235
9	0.0244	0.0255	0.0251	0.0246	0.0247	−0.0294	−0.0304	−0.0302	−0.0221	−0.0268
10	0.0252	0.0270	0.0281	0.0248	0.0249	−0.0289	−0.0284	−0.0019	−0.0219	−0.0246
11	0.0251	0.0272	0.0274	0.0250	0.0250	−0.0253	−0.0252	−0.0239	−0.0232	−0.0249
12	0.0264	0.0259	0.0263	0.0251	0.0252	−0.0247	−0.0243	−0.0239	−0.0281	−0.0241
13	0.0244	0.0266	0.0264	0.0246	0.0246	−0.0335	−0.0310	−0.0329	−0.0202	−0.0274
14	0.0266	0.0292	0.0276	0.0249	0.0248	−0.0276	−0.0274	−0.0289	−0.0206	−0.0265
15	0.0268	0.0308	0.0318	0.0250	0.0251	−0.0263	−0.0259	−0.0370	−0.0347	−0.0262
16	0.0263	0.0330	0.0338	0.0254	0.0255	−0.0198	−0.0214	−0.0202	−0.0309	−0.0250

Table 6 Positive and negative ideal solutions

	H_3BO_3	HCl	NaOH	Conversion to acid	Conversion to base	$\sum$ impurity in acid	$\sum$ impurity in base	Current efficiency	Energy consumption	Running Time
$\mathcal{S}^+$	0.0268	0.0330	0.0338	0.0254	0.0255	− 0.0335	− 0.0335	− 0.0019	− 0.0347	− 0.0274
$\mathcal{S}^-$	0.0236	0.0163	0.0158	0.0246	0.0246	− 0.0168	− 0.0156	− 0.0370	− 0.0188	− 0.0225

Table 7 Positive and negative ideal solutions

Exp. No	$\mathcal{D}_i^+$	$\mathcal{D}_i^-$	$\mathcal{T}_i$	Rank
1	0.3081	0.1872	0.3779	16
2	0.3078	0.1877	0.3788	15
3	0.3073	0.1886	0.3803	14
4	0.3020	0.1969	0.3946	13
5	0.2826	0.2239	0.4421	12
6	0.2767	0.2311	0.4551	11
7	0.2737	0.2346	0.4616	10
8	0.2707	0.2382	0.4681	9
9	0.2623	0.2473	0.4853	8
10	**0.1997**	**0.3002**	**0.6006**	**1**
11	0.2593	0.2505	0.4914	7
12	0.2558	0.2541	0.4984	5
13	0.2565	0.2534	0.4969	6
14	0.2556	0.2543	0.4987	4
15	0.2368	0.2718	0.5344	3
16	0.2257	0.2811	0.5546	2

The bold letters show the abreviation of technique for order preference by similarity to an ideal solution (TOPSIS)

energy consumption seriously. The smallest electrolyte concentration allows the minimum energy consumption. The adverse effect of current on energy consumption and process time indicates that the current at the maximum level makes the energy consumption minimum by decreasing the running time.

Increasing salt concentration increases the processing time, which leads to increased energy consumption. Increasing electrolyte concentration increases ionic conductivity in the anolyte and catholyte compartments, and this leads to accelerated reactions on the cathode and anode surface and faster consumption of protons and hydroxyl ions formed in the bipolar membranes. This both accelerates ion transport and reduces the effects of common ion transport and back diffusion, leading to increased salt conversion and reduced energy consumption.

Current efficiency

The effects of five experimental parameters on S/N values for current efficiency are presented in Fig. 7. Compared to electrolyte concentration, initial feed concentration, current, and initial acid and base concentration seem to be much more efficient. Current efficiency is an important criterion that shows the amount which is the fraction spent for the desired product of energy consumed in BMED. As seen in Fig. 7, feed concentration and electrical current have a significant effect on this criterion. Since current efficiency is a function of initial acid and base concentrations and electrical current, situations that contribute positively to conversion

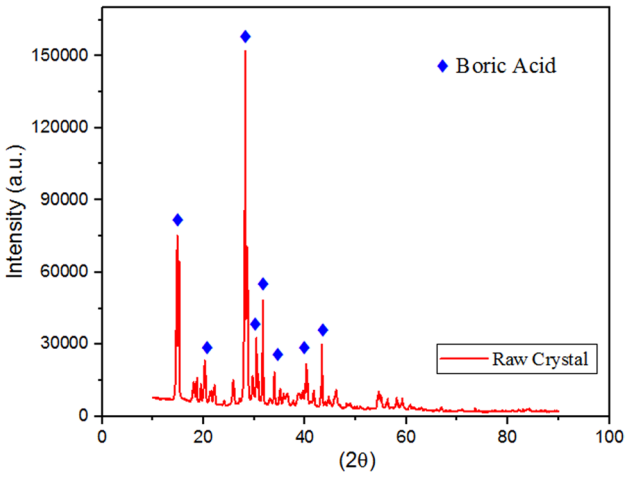


Fig. 8 X-ray diffractogram of produced boric acid crystals

also increase electrical efficiency. With increasing feed concentration, the processing time increases, enhancing common ion transport and back diffusion of products. This leads to a decrease in conversion and current efficiency. Increasing electrical current shortens the processing time leading to a decrease in common ion transport and back-diffusion of products. In summary, conditions that decrease common ion transport and back diffusion of products increase current efficiency (Ibáñez et al. 2013; Ghyselbrecht et al. 2014; Li et al. 2016; Kanca et al. 2022).

TOPSIS results

The first step of TOPSIS is the decision matrix formation given in Table 4. After the normalized decision matrix was formed by using Eq. (10), it was multiplied by the weight fraction (0.1) to form the weighted normalized decision matrix. The weighted normalized decision matrix is given in Table 5. Equations (11 and 12) were used to calculate positive ideal $(\mathcal{S}^{+})$ and negative ideal $(\mathcal{S}^{-})$ solutions, which were summarized in Table 6. The distance from positive ideal $(\mathcal{D}_i^{+})$ and negative ideal $(\mathcal{D}_i^{-})$ solutions was calculated by the Euclidian distance approach. The relative distance $(\mathcal{T}_i)$ from the ideal negative solution to the ideal positive solution determines the rank of the experimental design. Since the highest relative proximity is the optimum experimental condition, experiment 10 in Table 7 indicates the optimum experimental conditions with the highest $\mathcal{T}_i$ (0.6006). Experiments 16 and 15 also follow the experiment 10 with the $\mathcal{T}_i$ values of 0.5546 and 0.5344, respectively. The 10th experiment is selected as the optimum operating conditions for all criteria. The experimental data obtained under these conditions are presented in Table 1.

Since the boric acid molecules in the solution are crystallized in a layered form during the crystallization process, the solution is trapped in the crystals. Therefore, the purity of crude boric acid obtained from conventional processes is in the range of 95–98%. The crude crystals are usually further purified by re-crystallization. Each purification creates a new waste and additional cost. 99% purity is reached by re-crystallization. In BMED, boric acid is simultaneously concentrated and purified in the feed. As the boric acid molecules concentrated in the feed are crystallized in the desalted solution, crystals with high purity are formed. The purity of boric acid crystals concentrated in the feed solution under optimum conditions is very high compared to the purity of boric acid obtained in conventional processes. X-ray patterns of the obtained boric acid crystals are given in Fig. 8, exploring the high purity of the boric acid crystals.

If boric acid and sodium hydroxide are produced from tincal by the process proposed in Fig. 1, the following advantages will arise compared to conventional processes. In industry, sodium hydroxide is commonly produced by treating NaCl with chlor-alkali process. In this production process, approximately 1 mol of chlorine gas containing O_2 and water vapor is formed per 1 mol of NaOH. The demand for NaOH in the industry is constantly increasing, but the same increase does not occur for chlorine gas. The fact that the chlorine gas produced by the chlor-alkali process cannot be supplied to the market like NaOH creates a need for chlorine-free sodium hydroxide production processes. While boric acid is produced from colemanite with sulfate acid in conventional processes, 0.33 mol of gypsum, which is solid waste, is formed with each mole of boric acid produced. The results obtained show that the process presented in Fig. 1 can produce boric acid with very high purity on an industrial scale without generating gypsum and it can produce NaOH on an industrial scale without generating chlorine. To the best of our knowledge, there is a study by Erkmen and Yapici that is directly related to our study. They investigated the production of H_3BO_3 and NaOH from borax solutions by electrodialysis. They produced boric acid having a purity of 99.52% and sodium hydroxide with a purity of 99.12% with a current efficiency between 93–99%. However the conversion of salt to products was about 19% which is quite low. In summary, as mentioned in the discussion section, if membranes can be synthesised in which the limitations such as water transport by electro osmosis and common ion transport in ion exchange membranes can be reduced, the proposed process can be commercialised in the near future.

Conclusion

Boric acid and sodium hydroxide are the most important raw materials for many industrial areas. The experiments were carried out to investigate BMED applicability for the simultaneous NaOH recovery, and H_3BO_3 enrichment in diluate. The findings of the experiments verified that BMED technique makes the H_3BO_3 and NaOH recovery possible without the formation of any solid waste and concentrated liquid waste. After the experiments were designed by Taguchi, TOPSIS which is a multiple decision-making analysis method was employed to determine the optimum experimental conditions. The results of TOPSIS analysis indicated that the 10th experiment represents the optimum experimental conditions. The optimum conditions were determined to be 160 g NaCl/L + 36 g H_3BO_3/L for the initial feed concentration (A), 4.2 A for the applied current (B), 31 L/h for the flow rate of the solutions (C), 0.15 M for the initial acid and base concentrations (D), and 0.2 M for the electrolyte concentration (E). BMED process can be modified to improve the H_3BO_3 purification under optimum process conditions. Furthermore, this developed process has the potential and advantage of producing NaOH on industrial scale without gaseous Cl_2 emission. Further research should be carried out, especially employing solutions with higher initial boric acid content in the feed.

Supplementary Information The online version contains supplementary material available at https://doi.org/10.1007/s13762-024-06044-2.

Acknowledgements This study was supported by The Scientific and Technological Research Council of Turkey (TUBITAK) under the project with Grant Number 218M777. The authors thank to TUBITAK

Author contributions Hülya Şenol: Material preparation, data collection and analysis, Duygu Adıgüzel: Material preparation, data collection and analysis, Arzu Kanca: Investigation; Writing—original draft preparation, Osman Nuri Ata: Conceptualization, Review and editing, Funding acquisition;, Supervision, Sinan Yapıcı: Investigation; Writing—original draft preparation.

Declarations

Conflict of interest The authors declare that they have no known competing financial interests or personal relationships that could have appeared to influence the work reported in this paper.

References

Ata ON, Kanca A et al.(2017) Optimization of ammonia removal from aqueous solution by microwave-assisted air stripping. Water Air Soil Pollut 228:1–10

Başkanlığı SGD (2018) Bor sektör raporu. Ankara

Behzadian M, Otaghsara SK et al.(2012) A state-of the-art survey of topsis applications. Expert Syst Appl 39(17):13051–13069

Bunani S, Arda M et al.(2017a) Effect of process conditions on recovery of lithium and boron from water using bipolar membrane electrodialysis (bmed). Desalination 416:10–15

Bunani S, Yoshizuka K et al.(2017b) Application of bipolar membrane electrodialysis (bmed) for simultaneous separation and recovery of boron and lithium from aqueous solutions. Desalination 424:37–44

Dursun L, Ata ON et al.(2021) Bipolar membrane electrodialysis for binary salt water treatment: valorization of type and concentration of electrolytes. Ind Eng Chem Res 60(5):2003–2010

Fu L, Gao X et al.(2014) Preparation of succinic acid using bipolar membrane electrodialysis. Sep Purif Technol 127:212–218

Gauri SK, Chakravorty R et al.(2011) Optimization of correlated multiple responses of ultrasonic machining (usm) process. Int J Adv Manuf Technol 53:1115–1127

Ghyselbrecht K, Silva A et al.(2014) Desalination feasibility study of an industrial nacl stream by bipolar membrane electrodialysis. J Environ Manag 140:69–75

Ibáñez R, Pérez-González A et al.(2013) Acid and base recovery from softened reverse osmosis (ro) brines. Exp Assess Using Model Conc Desalin 309:165–170

Jiang C, Wang Q et al.(2015) Water electro-transport with hydrated cations in electrodialysis. Desalination 365:204–212

Kackar RN (1985) Off-line quality control, parameter design, and the taguchi method. J Qual Technol 17(4):176–188

Kanca A, Şenol H et al.(2022) Boric acid recovery in dilute during the desalination process in bmed system. Desalination 538:115920

Li Y, Shi S et al.(2016) Bipolar membrane electrodialysis for generation of hydrochloric acid and ammonia from simulated ammonium chloride wastewater. Water Res 89:201–209

Nagasawa H, Iizuka A et al.(2011) Utilization of bipolar membrane electrodialysis for the removal of boron from aqueous solution. Ind Eng Chem Res 50(10):6325–6330

Noguchi M, Nakamura Y et al.(2018) Simultaneous removal and recovery of boron from waste water by multi-step bipolar membrane electrodialysis. J Water Process Eng 23:299–305

Öner M, Ata O et al.(2023) Bipolar membrane electrodialysis for mixed salt water treatment: determination of optimum conditions by topsis-based taguchi method. Int J Environ Sci Technol 20(1):587–604

Özdagoglu A (2013a) Farkli normalizasyon yöntemlerinin topsis'te karar verme sürecine etkisi/the effects of different normalization methods to decision making process in topsis. Ege Akademik Bakis 13(2):245

Özdagoglu A (2013b) Farklı normalizasyon yöntemlerinin topsis'te karar verme sürecine etkisi. Ege Akad Bakış 13(2):245–257

Panda M, Jagadev AK (2018) Topsis in multi-criteria decision making: a survey. In: 2018 2nd International conference on data science and business analytics (ICDSBA), IEEE, pp 51–54

Pignatiello JJ Jr (1988) An overview of the strategy and tactics of taguchi. IIE Trans 20(3):247–254

Rottiers T, Ghyselbrecht K et al.(2014) Influence of the type of anion membrane on solvent flux and back diffusion in electrodialysis of concentrated nacl solutions. Chem Eng Sci 113:95–100

Sun X, Lu H et al.(2017) Recovery of citric acid from fermented liquid by bipolar membrane electrodialysis. J Clean Prod 143:250–256

Tanaka Y (2004) Overall mass transport and solution leakage in an ion-exchange membrane electrodialyzer. J Membr Sci 235(1–2):15–24

Tolun R, Emir B, Kalafatoglu E, Kocakus S, Yalaz N (1981) Boric acid and sodium hydroxide production from tincal concentrate by electrolysis method. In: TUBITAK Marmara Research Center, Chemistry Department, Project No: 0718018001

Tong K, Kwong CK et al.(2003) Optimization of process conditions for the transfer molding of electronic packages. J Mater Process Technol 138(1–3):361–365
Tong L-I, Wang C-H et al.(2004) Dynamic multiple responses by ideal solution analysis. Eur J Oper Res 156(2):433–444
Tong L-I, Wang C-H et al.(2005) Optimization of multiple responses using principal component analysis and technique for order preference by similarity to ideal solution. Int J Adv Manuf Technol 27:407–414

Springer Nature or its licensor (e.g. a society or other partner) holds exclusive rights to this article under a publishing agreement with the author(s) or other rightsholder(s); author self-archiving of the accepted manuscript version of this article is solely governed by the terms of such publishing agreement and applicable law.

Authors and Affiliations

H. Şenol[1] · D. Adıgüzel[1] · A. Kanca[1] · O. N. Ata[1] · S. Yapıcı[2]

✉ O. N. Ata
oatar@atauni.edu.tr

[1] Chemical Engineering Department, Atatürk University, 25240 Erzurum, Turkey

[2] Chemical Engineering Department, İnönü University, 44280 Malatya, Turkey